CHT ANALYSIS OF THE TIP SEAL OF THE COUNTER ROTATING LP TURBINE

Włodzimierz WRÓBLEWSKI, Krzysztof BOCHON

Institute of Power Engineering and Turbomachinery, Silesian University of Technology, Gliwice, Poland
E-mail: krzysztof.bochon@polsl.pl

Abstract

Much emphasis in aviation is put on reducing pollutant emissions and fuel consumption. It is mainly associated with an increase of the turbine cycle efficiency, e.g. by minimizing the internal leakages.

The aim of the study was to examine the phenomena connected with leakage flow through the tip seal and CHT analysis of the whole tip area of the blade including part of casing, with rotating cavity above the seal.

The CFD analyses were performed using the commercial software ANSYS-CFX. For the complicated geometrical configuration of the seal region a calculation model was proposed which enabled a satisfactory approach of flow and heat transfer phenomena. The mesh for the blade to blade channel was generated as fully structural. For the remaining parts the extruded hexa-dominant mesh was generated. Calculations were performed using the Shear Stress Transport turbulence model. The ideal gas properties were assumed. The CHT analyses were performed for two cases characterized by different thermal conductivity of the metal. At the outer surface of the solid domain a forced convection is assumed.

Fluid flow parameters which allowed to recognize flow structures, losses and mixing were taken into account. In CHT analyses the flow structures for the cavity and the heat transfer conditions were obtained. Also the temperature distribution in the whole domain was considered.

Key words: CFD, tip seal, honeycomb, Conjugate Heat Transfer

INTRODUCTION

To ensure reliable operation of the turbine, adequate clearances should be retained between rotating elements. The clearances are greater, the greater the leakage flow and consequently, higher energy losses. So it is important to look for seals solutions, which allow for safe operation of the turbine with the least loss of energy.

The most common seals in the steam and gas turbines are labyrinth seals, mainly because of their simplicity, low cost, reliability, material selection flexibility, lack of pressure limitations and tolerance to thermal variations. They are often combined with honeycomb land.

The honeycomb seal withstands high temperatures and high rotational speeds, while allowing limited rubbing of the stator fins at the rotor without the danger of seal failure. Therefore, a significantly tighter seal clearance, which represents a leakage-reducing factor, can be realized (Li *et al.*, 2007).

Many researches were performed over labyrinth seals. An example of a general assessing of the impact of leakage on the turbine performance is a study presented by (Cherry *et al.*, 2005). The efficiency of analyzed turbine, after taking into account gaps and seals, decreased

by 0.6% in comparison with the simplified case. Much attention was also paid to the evaluation of the impact of seals configuration on the leakage and seals modifications in order to reduce leakage e.g. (Vakili *et al.*, 2005).

Leakage flux, which bypasses the blade-to-blade channel and does not perform work at this point, has the largest impact on losses generated by the seal. But this is not the only component that causes the loss in the seal. Rosic and Denton (2006) estimated the impact of the different mechanisms of losses generation by the shroud leakage on the turbine efficiency. Beyond the leakage flux, which bypasses the blade-to-blade channel, great impact on losses generation has the mixing process of the re-entering leakage flux with the main flow. The other losses mechanisms are connected with the existence of the inlet and outlet cavity and shroud windage. The contribution of each component in the losses generation, however, will depend on the seal construction.

Interactions between the re-entering leakage and the main flow were widely analysed e.g. (Anker and Mayer, 2002, Giboni et al., 2004). Modifications of the seal in order to limit the influence of the re-entering leakage on the main flow were analysed in (Adami *et al.*, 2007, Rosic *et al.*, 2007, Rosic and Denton, 2006).

The honeycomb seals play nowadays more important role. They are widely used in turbomachinery because of many advantages. They can withstand hard working conditions at high temperatures and high speeds, while allowing for limited rubbing without the danger of damaging the seal (Rudolph *et al.*, 2009). It allows for using smaller clearances and in consequence for reducing the leakage.

The honeycomb seals were the subject of numerous studies. Major role in this field play numerical calculations. Choi and Rode (Choi and Rode, 2003) used a 3D model replacing the honeycomb cells with circumferential grooves. Recent investigations have shown a greater possibility of flow structure modelling. A complete geometrical representation of the honeycomb cells was considered by Soemarwoto et al. (Soemarwoto *et al.*, 2007). They used a 3D mesh with over 10 million cells. Fine grids of this kind which take into account honeycomb structure can sufficiently capture the important flow features with high gradients around the knife-edge and in the swirl regions. Complete geometrical representation of the honeycomb cells was also used by Li et al. (Li *et al.*, 2007) They considered the axial flow through the three knives configuration with stepped honeycomb land. The influence of the pressure ratio and of the sealing clearance on the leakage flow rate was investigated. In case of non-rotating honeycomb labyrinth seal, the influence of free space in the honeycomb cell above seal fin was observed, resulting in an increased leakage flow rate. Similar leakage flow rate was obtained for rotating and non-rotating honeycomb labyrinth seal.

Moreover in literature can be found many examples of analysis of different configurations and modifications of labyrinth seals with honeycomb land, to improve its efficiency e.g. (Chougule *et al.*, 2008, Kang *et al.*, 2010, Wróblewski *et al.*, 2010). Kang *et al.* noticed, that honeycomb enlarged leakage flow rate for all considered seal configurations and seal clearances, but the leakage flow rate was decreasing with decreasing clearance.

Despite of increased leakage flow rate for the labyrinth seal with honeycomb land, this solution is used more frequently, both in new designs as well during the modernization. This is mainly caused by the possibility of safe seal clearance reduction, what finally allows reducing the leakage flow rate.

The aim of the study was to examine the phenomena connected with leakage flow through the tip seal and CHT analysis of the whole tip area of the blade including: seal area, rotating cavity above the seal, the tip part of the blade to blade channel and solid domain. The analyses were performed using ANSYS CFX tools.

GEOMETRY MODEL DEFINITION AND MESH

The CFD analyses were performed using the commercial software ANSYS-CFX. The area of the interest concerns the tip part of the LP turbine rotor blade of the aircraft engine. It is complex and large in relation to scales of phenomena that occur, therefore very important role played definition of the calculation domain and the mesh quality. The model for the CHT analysis consisted of four independent domains (Fig. 1b); three for the fluid, including the blade-to-blade domain, the seal domain, the domain of the drum cavity, and one domain for the solid. The solid multicomponent domain is reduced to a single domain, and the real shape is simplified (Fig. 1a) to reduce the number of computational meshes and domain interfaces. Each domain involved in the CHT analysis is defined with an individual pitch corresponding to the geometry configuration and the physical phenomena periodicity. The solid domain is as thick as the seal area, following the honeycomb pitch. The drum cavity was built as a domain extended in the circumferential direction by five degrees. This value was selected after some preliminary studies in which calculations for the cavity domain were performed using different periodicity definitions. The periodicity definition for the blade-to-blade depends on the blade pitch.
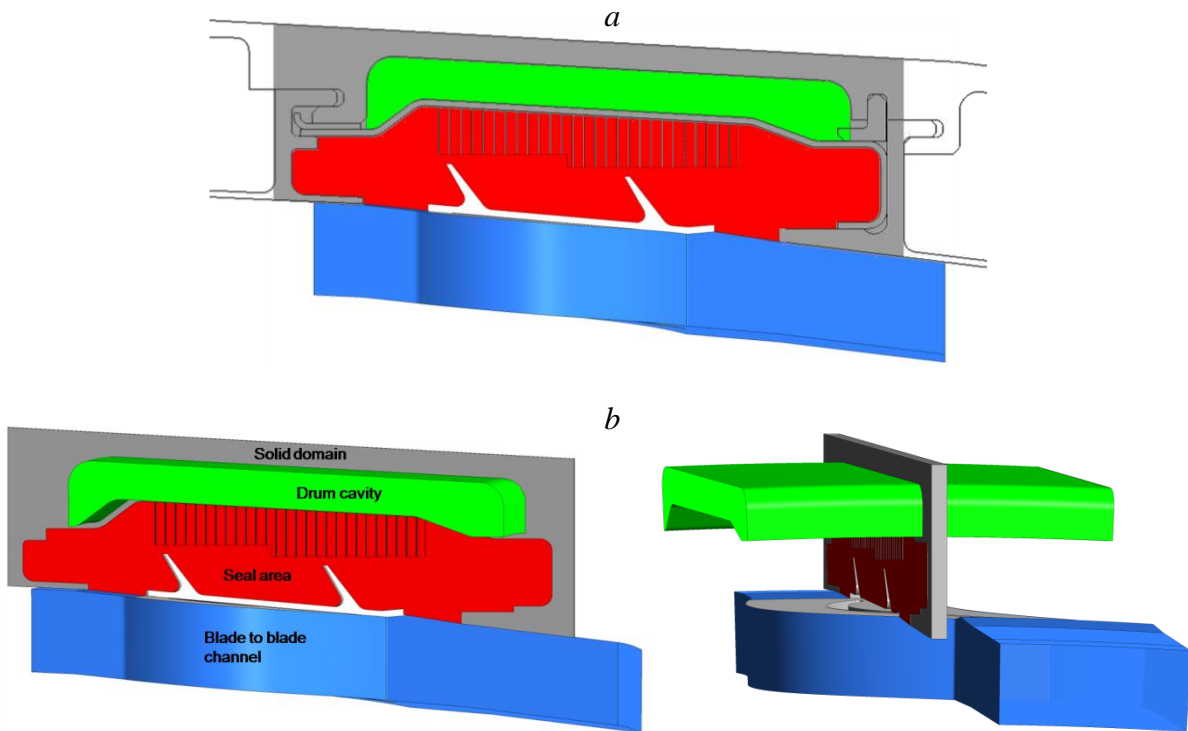

Fig. 1 Geometrical model for CHT analysis: a. solid shape simplification, b. definition of numerical domains

The mesh for the blade-to-blade channel was generated as fully structural and consisted of about 2M nodes. For the remaining parts the extruded hexa-dominant mesh was generated. The sizes of meshes for particular domains were as follows: for the seal domain – 4.4M nodes, for the solid domain – 30k nodes, and for the cavity – 750k nodes. The total number of nodes is about 7M. All the meshes for fluid domains have y+ values less than 2, but in the vast majority of the calculation area it was less than 1. Higher values occurred near the fins tips and on the bottom surface of the honeycomb land.

The relationships between individual domains are defined using appropriate fluid-fluid or fluid-solid interfaces. For the connection between the domain of the blade-to-blade channel and the seal domain, the fluid-fluid type interface was used with the frozen rotor option. Beside these interface, the interfaces between the solid domain and domains for the blade-to-

blade channel, the seal area and the drum cavity were defined. The solid domain and the cavity domain are rotating domains with rotational speed of ω=-839 rpm, like the seal domain. Consequently, the interface between the solid domain and the seal domain, whose pitches are the same, is defined without pitch change. The solid domain and the cavity domain have different pitches, and therefore the frozen rotor option for the interface has to be implemented.

PHYSICAL MODEL AND BOUNDARY CONDITIONS

Total pressure, total temperature and the flow angle distribution were applied at the inlet (Fig. 2) as functions of the blade height. The radial distribution of the circumferentially averaged static pressure was used as a boundary condition at the outlet. Table 1 presents the average parameters in the main flow, which refer to the plane at the position of the blade trailing edge in the previous row (TE), and the plane at the position of the blade leading edge in the next row (LE). The parameters correspond to the results of the main flow path computations for the turbine. For the main flow at the inlet, the turbulence intensity Tu was assumed to be 5%.

The symmetry condition was used at the bottom wall of the channel. Periodic boundary conditions were applied to both sides of each calculation domain in order to take into account the 3D structure of the flow. The rotating speed of $\omega = 839$rpm was applied to the blade-to-blade channel domain. The domain for the seal area rotates in the opposite direction at rotating speed of $\omega = -839$rpm.

Table 1 Main flow parameters applied to CFD model definition

TE (previous row)					LE (next row)
Total Pressure (Absolute)	Total Temperature (Absolute)	α=arctan (v_t/v_{ax})	Static Pressure	Mach	Static Pressure
kPa	K	^{o}	kPa	-	kPa
58.51	699.08	-62.74	55.28	0.291	51.55

All considered domains are periodic. The vertical surfaces of the solid domain are assumed as adiabatic walls. At the outer surface of the solid domain a forced convection is assumed with bulk temperature $T = 288$K, which corresponds to ambient temperature at the ground level. The heat transfer coefficient is calculated assuming simplified relations as $h = 130$W/(m^2 K).

The gas properties were set up as air ideal gas with the total energy heat transfer option. Molecular viscosity and conductivity were specified as a function of static temperature according to Sutherland's formula. The specific heat at constant pressure was specified as a function of temperature with the formula:

$$c_p = 0.0003T^2 - 0.1217T + 1014.4 \text{ , kJ/(kg K)} \tag{2}$$

The drum material is assumed as stainless steel with constant density of 7900 kg/m^3 and specific heat of 585.2 J/kg/K. Two cases with different definitions of thermal conductivity K are examined. In the first case – (Case I), the thermal conductivity is relatively low, and it is specified as:

$$K = 0.0182T + 6.13, \text{ W/(m K)} \tag{3}$$

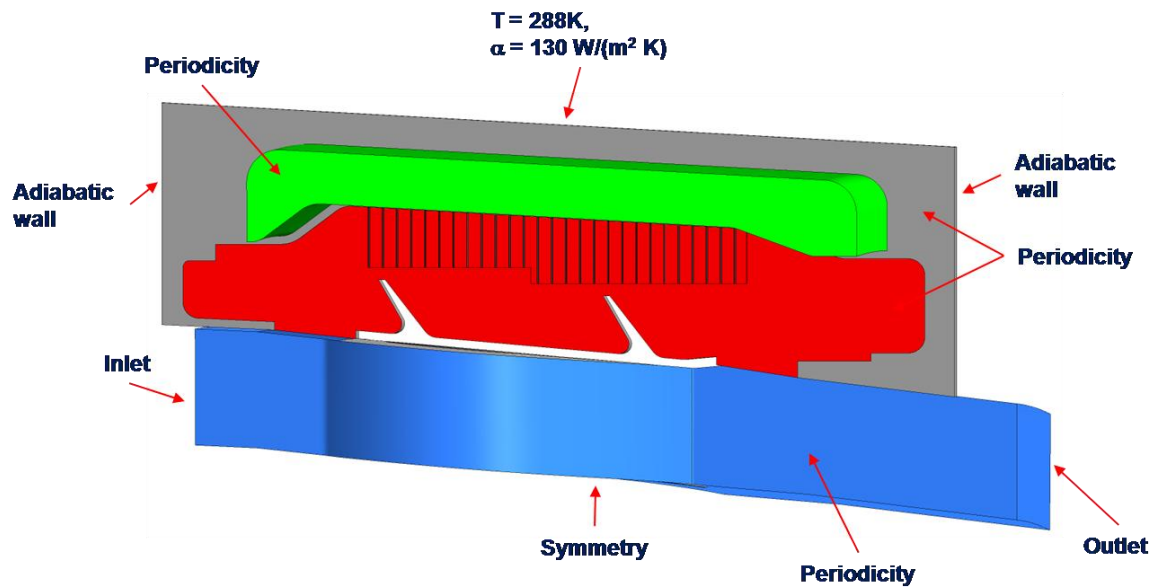and in the second case – (Case II), the constant value $K = 40$W/(m K) is set.

Fig. 2 Overview of boundary conditions for CHT analysis

A high resolution advection scheme was set up for the continuity, energy and momentum equations. Similarly for the turbulence eddy frequency and the turbulence kinetic energy equations high resolution option was specified. Calculations were performed using the Shear Stress Transport turbulence model with the Kato-Launder production limiter and the curvature correction.

NUMERICAL ANALYSIS

Analysed tip seal with the honeycomb land is characterised by the complex geometry and complex flow phenomena. The complex flow structures are characterised by high velocity flows over the fins, large velocity gradients, turbulence and intensive energy dissipation. Important role in modelling of the flow through the considered seal plays also counter-rotating construction of the engine where the rotations of the rotor and casing are in opposite directions.
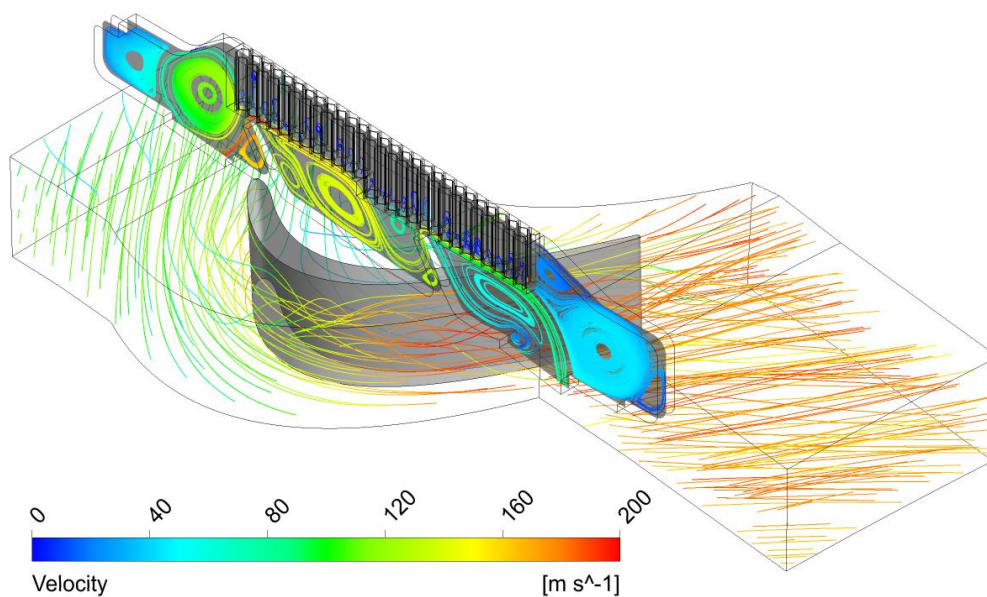

Fig.3 Streamlines plot

Fig. 3 presents the streamlines plot for the analyzed geometry. They are the combination of three-dimensional streamlines in the blade-to-blade channel and surface streamlines in the seal area. The colour of the streamlines refers to the velocity in the relative frame of reference.

The leakage path in the seal area is relatively complex. The geometrical configuration of the seal favour the inflow of leakage flow at a sharp angle to the fins, what enlarges the contraction. Moreover significant curvature of the main path of leakage and nearly perpendicular inflow of the leakage on the honeycomb land causes the slowing down of the flow and leakage reduction.
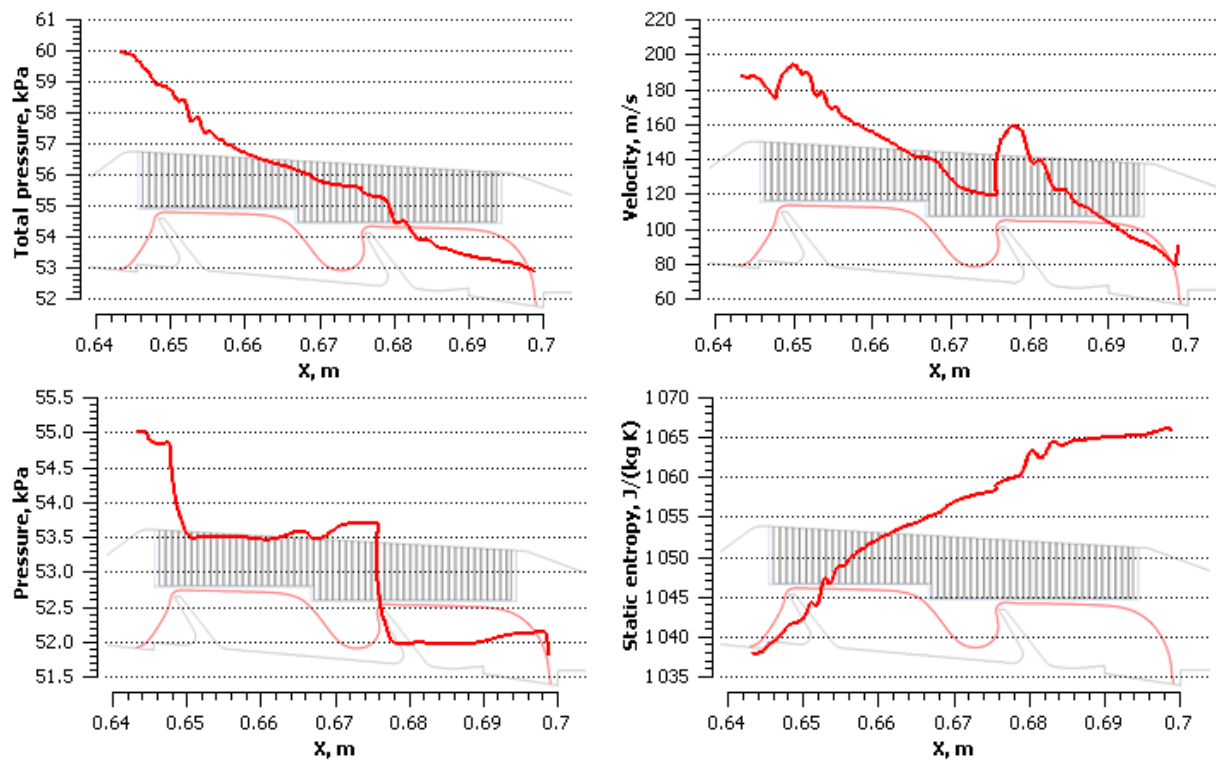
Fig. 4 Parameters distribution along the leakage streamline

Fig.3 presents distribution of selected parameters along the leakage streamline. Because of loses in the seal, average values of the total pressure, static pressure and velocity are decreasing along the streamline, whilst the value of static entropy increases.

The total pressure as well as velocity is defined in the relative frame of reference. The static pressure in particular cavities doesn't change significantly. Its rapid decrease is observed on the seal fins, where the flow speeds up. In the cavity the velocity of the leakage flow is decreasing.

The flow through the gaps above the fins, where significant contraction of the stream takes place, leads to the parameters fluctuations close to the honeycomb. It is visible on charts, especially of total pressure and static entropy. The fluctuations die away further in the flow. The phenomena can be observed also in Fig. 5 – 7, which present distribution of total pressure, static entropy and turbulence kinetic energy in the seal area. The fluctuations are visible behind fins, close to the honeycomb.

Fig. 5 presents the total pressure distribution in the seal area. The leakage path through the seal is clearly visible. As in Fig. 4, one can observe the total pressure drop along the leakage path, what is connected with the energy dissipation. The largest drop is observed in the inlet chamber of the seal and behind fins.
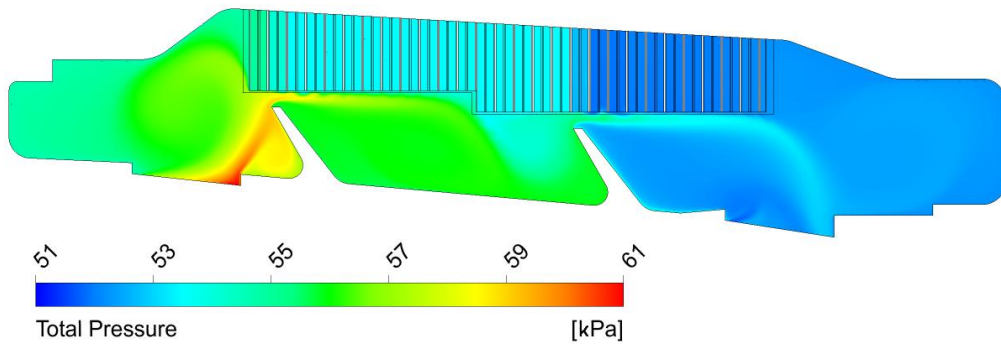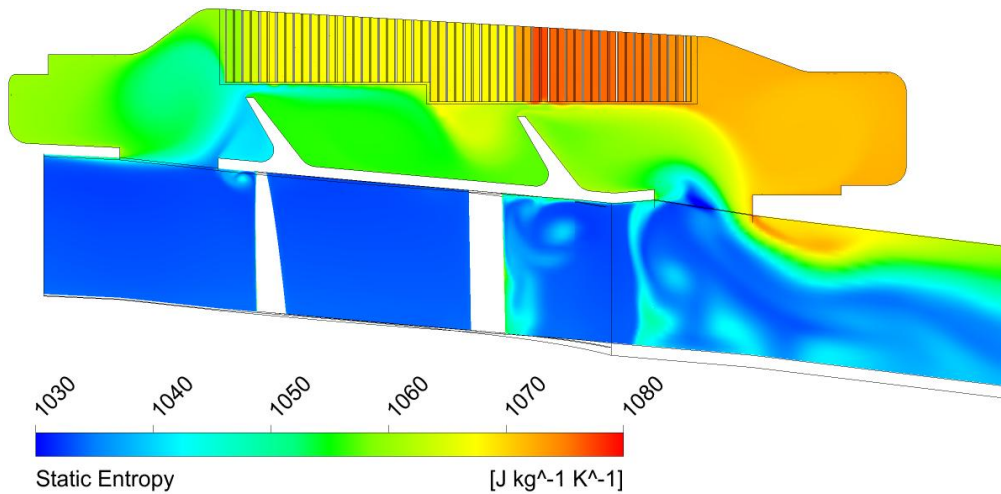
Fig. 5 Total pressure distribution in the tip seal

Fig.6 Static entropy distribution in the tip seal

Distribution of entropy in calculation domain is shown in Fig. 6. The entropy distribution shows the places where losses are generated e.g. due to the turbulence. They are also visible in Fig. 7, where turbulence kinetic energy is presented. Besides losses in the seal, a small increase of the entropy and turbulence kinetic energy can be observed in the main flow, behind the seal inlet, where small vortex is formed. Large changes can be observed in the seal outlet area and behind the outlet, where the leakage interacts with the main flow.
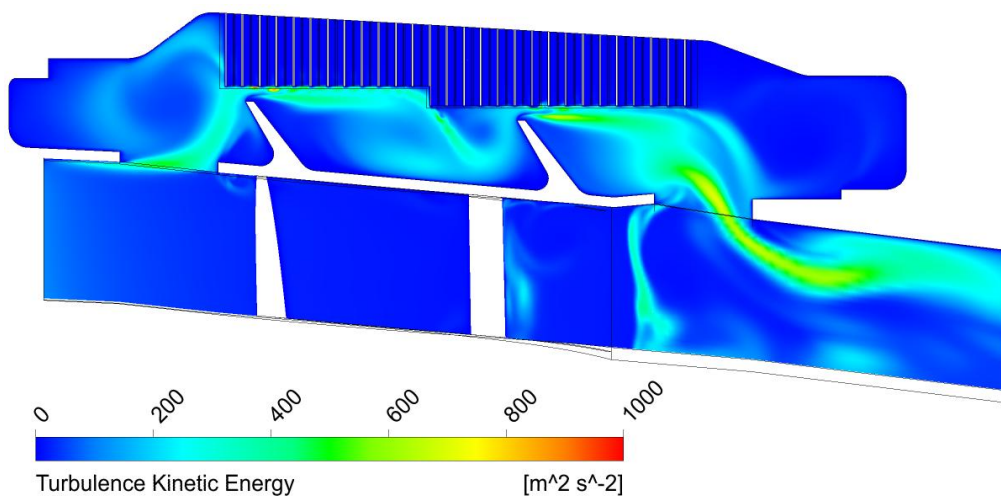

Fig. 7 Turbulence kinetic energy distribution in the tip seal

An overview of the temperature distribution in the analysed area is presented in Fig. 8 for Case I and in Fig. 9 for Case II. The temperature distribution in the solid and the seal area is influenced by: temperature distribution in the blade-to-blade channel and in the seal, as well as by the assumed environment parameters and material properties of steel. Due to the lower value of thermal conductivity in Case I we have to deal with lower temperatures in the upper part of the solid and with greater temperature gradient.
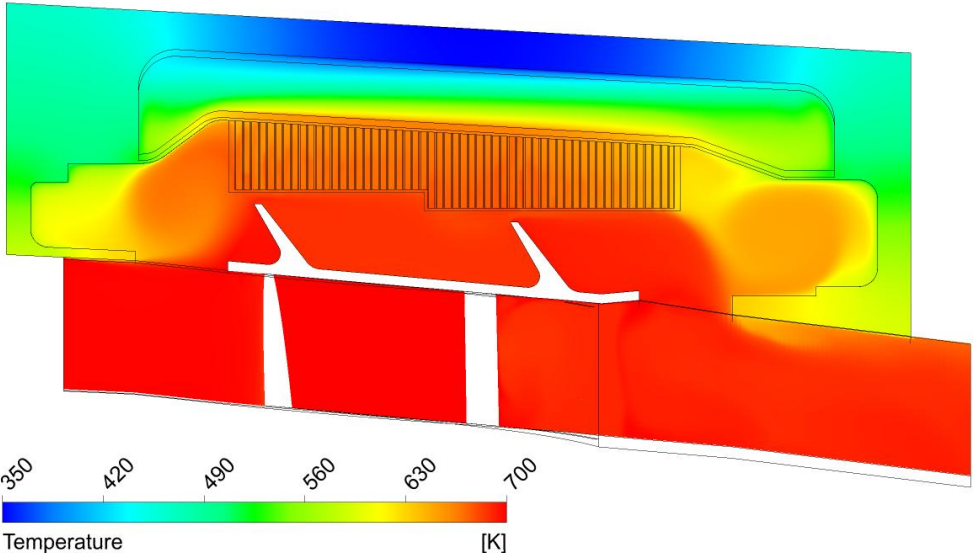

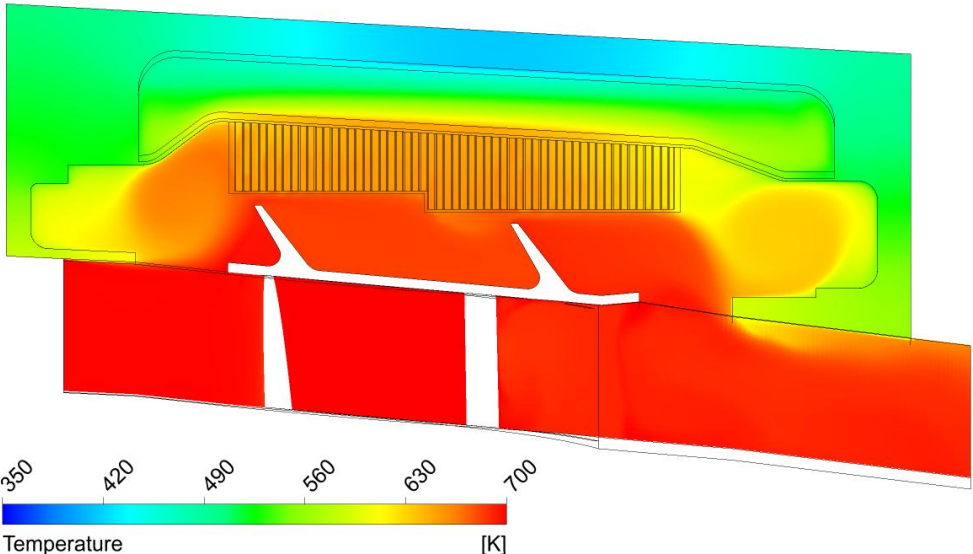*Fig. 8 Temperature contour from CHT results (Case I)*

Fig. 9 Temperature contour from CHT results (Case II)

In the cavity above the seal stratified temperature distribution can be observed, which is determined by the temperature difference between the seal area and the area outside the casing. Analyzing Fig. 8 and 9 can be concluded that an important role in the heat exchange between the casing elements of the engine, the cavity, and the seal plays the honeycomb. In the region of the honeycomb the largest temperature differences are observed, resulting from different values of thermal conductivity. Heat transfer in the honeycomb affects also the lower temperature level in the chamber on the outlet of the seal, what is visible in Fig. 9. The temperature difference for Case I and II in the chamber above the inlet to the seal is less

noticeable. Cooling of the solid domain by the outer region does not have a significant effect on the seal area.
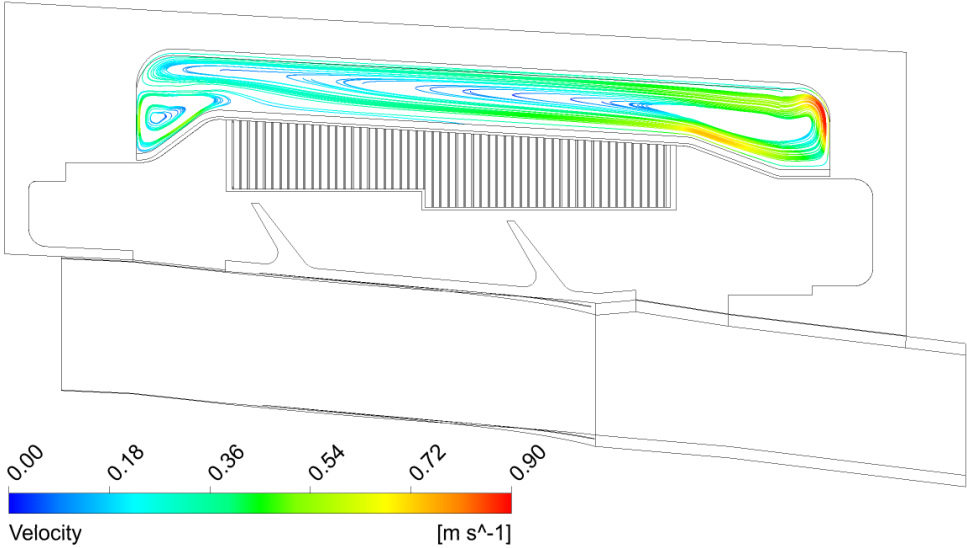

Fig. 10 Streamlines plot in the drum cavity

Fig. 10 shows the streamline plot in the cavity. The main vortex is stretched along the whole cavity width. In the left part of the cavity there is an additional small vortex created, that fills the gap on the left side of the cavity. The streamlines are coloured according to velocity values in relative frame of reference. The intensity of air movement in the chamber is small, as indicated by very low speed, not exceeding 1m/s. This is due to low intensity of heat transfer by convection. A small intensity of convective motions in the cavity can also be observed in Fig. 8 and 9.

Small importance of the convective motions is caused by the dominant role of the radial temperature distribution. The cooler and denser air is located in the top part of the cavity, so the centrifugal force does not cause movement of gas. The temperature difference in the axial direction is so small, that there is no major impact on the movement of air in the cavity. Important rule in limiting the possible convection have also small height of the cavity.
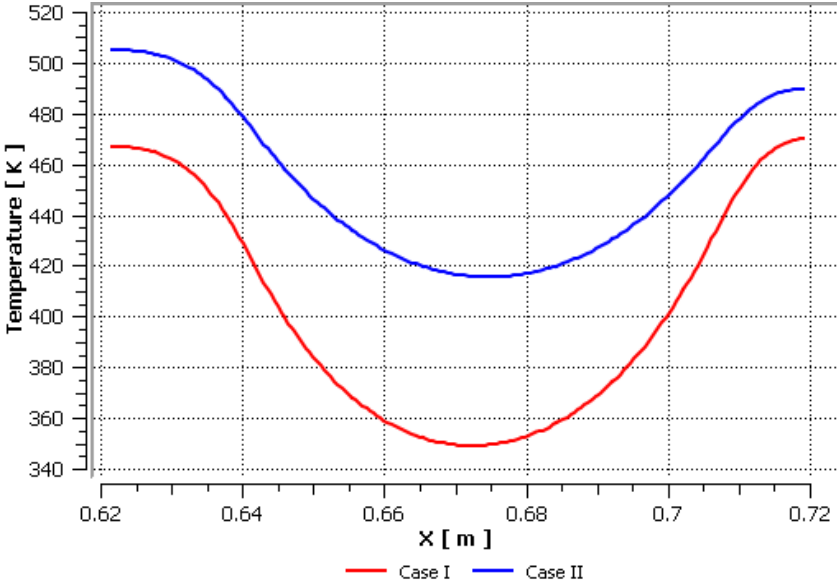

Fig. 11 Temperature distribution in metal along the outer wall

Fig. 11 presents the temperature distribution on the outer surface of the casing. The maximum temperature difference on the outer wall is calculated at about 120K for Case I and 90K for Case II. The temperature of the outer surface does not exceed 510K in Case I and 470K in Case II.

A similar comparison is presented in Fig. 12, which shows the temperature distribution in the radial direction on the left side of the model, on the adiabatic surface. For the lowest value of the radius the temperatures are the same, because of the same boundary condition on the bottom surface of the solid. Different values of the heat conductivity coefficient cause that the temperatures differ in the remaining part of the surface and the difference increases with the increase if the radius value. The highest difference of about 40K is at the top of the surface.
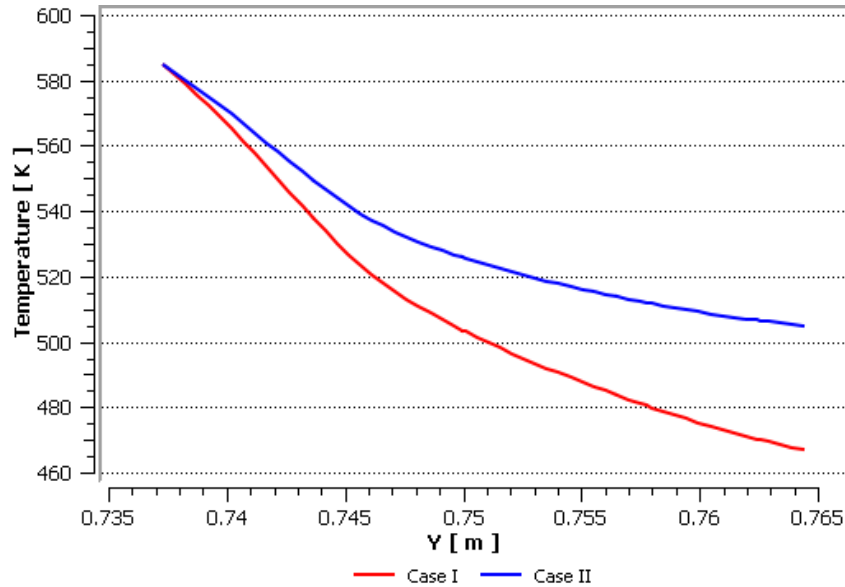

Fig. 12 Temperature distribution in metal in the radial direction

According to the rotating cavity the Nusselt number is defined as [48]:

$$\mathrm{Nu} = \frac{q \cdot b / 2}{k \cdot \Delta T}, \tag{4}$$

where: where q is the heat flux, b is the cavity width, k is the thermal conductivity and ΔT is the temperature difference. The temperature difference in rotating cavity analysis is generally defined as the difference between the temperature of the heated surface and the inlet temperature of the cooling air for the open cavities, and as the temperature difference between heated and cooled surface for the closed cavity. So this is the difference between the highest and lowest temperature in the cavity. The same approach was used in considered case.

For the assumed conditions the average value of Nusselt number on the cavity walls for Case I was Nu = 5.28, whilst for Case II Nu = 5.75. Distribution of Nusselt number is presented in Fig. 13. The highest value of it on the bottom wall of the cavity is located in the area of the arc on the left hand side of the cavity. On the top surface the maximum value of Nusselt number is located near the right hand side of the cavity. Information about heat transfer conditions can be useful for conducting more detailed calculations of thermal resistance of the structure.
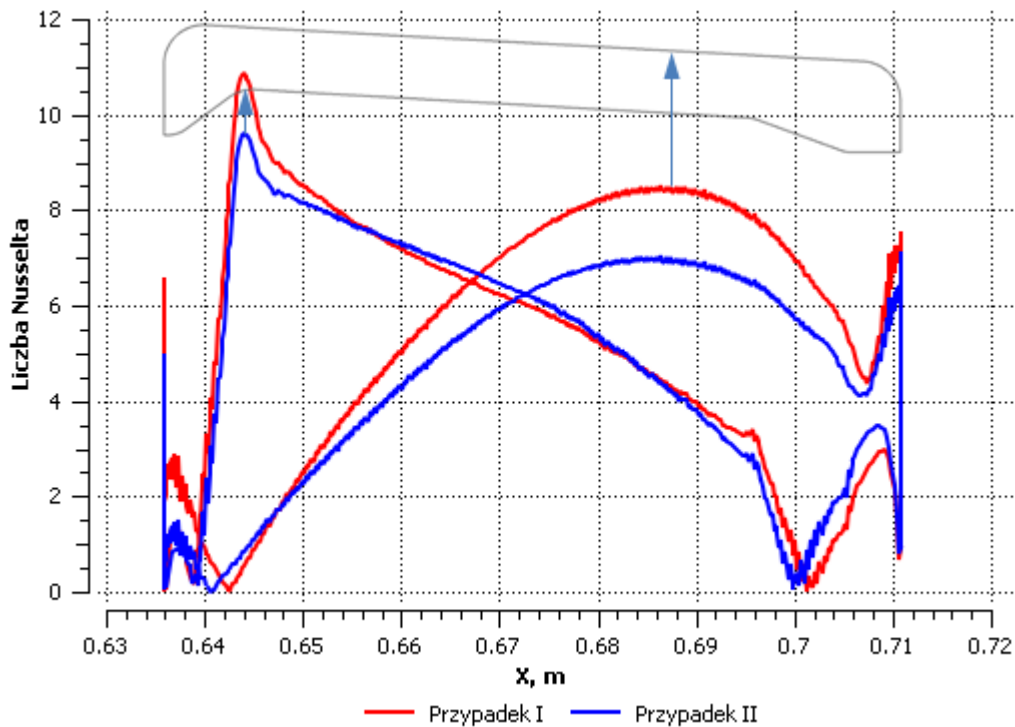
Fig. 13 Nusselt number distribution around the cavity for the fixed temperature difference

CONCLUSIONS

The aim of the study was to examine flow phenomena of the leakage flow through the tip labyrinth seal with honeycomb land in the low-pressure counter-rotating turbine and to perform the CHT analysis of the seal area with a part of the casing and the drum cavity.

The calculation domain is relative large and complex, therefore many attention was paid to prepare geometry and mesh. The calculation domain definition method for the rotor blade tip zone was proposed in order to conduct the CHT analysis. Calculations were performed for air ideal gas, where molecular viscosity, thermal conductivity and specific heat at constant pressure were specified as a function of temperature.

The main parameters and flow structures of the leakage flow were characterised. There are small fluctuations of parameters observed near the honeycomb land, behind fins. The area behind fins is also place were larger energy dissipation is observed. The other places where higher energy losses were observed are: the inlet chamber, the area near the seal outlet in the outlet chamber and the main flow where mixing takes place.

The flow structures for the cavity and the heat transfer conditions were obtained. Also the temperature distribution in the whole domain was considered. A relatively weak forced convection in the cavity was detected, caused by the higher temperature of the inner surface of the cavity, lower of the outer surface and relatively small radial size of the cavity. The difference of the thermal conductivity changes the temperature distribution in the solid, cavity and near the honeycomb. Determined heat transfer conditions can be used further in the strength analyses.

REFERENCES

Adami P., Martelli F., Cecchi S., (2007): *Analysis of the Shroud Leakage Flow and Main Flow Interactions in High-Pressure Turbines Using an Unsteady CFD Approach*, Proceedings of the European Conference On Turbomachinery ETC2007-165

Anker J. E., Mayer J. F., (2002): *Simulation of the Interaction of Labyrinth Seal Leakage Flow and Main Flow in an Axial Turbine*, ASME Paper GT2002-30348

Giboni A., Wolter K., Menter J. R., Pfost H., (2004): *Experimental and Numerical Investigation into the Unsteady Interaction of Labyrinth Seal Leakage Flow and Main Flow in a 1.5-stage Turbine*, ASME Paper GT2004-53024

Li J., Yan X., Li G., Feng Z., (2007): *Effects of Pressure Ratio and Sealing Clearance on Leakage Flow Characteristics in the Rotating Honeycomb Labyrinth*, ASME Paper GT2007-27740

Cherry D., Wadia A., Beacock R., Subramanian M., Vitt P., (2005): *Analytical Investigation of a Low Pressure Turbine With and Without Flowpath Endwall Gaps, Seals and Clearance Features*, ASME Paper GT2005-68492

Choi D. C., Rhode, (2003): *Development of a 2-D CFD Approach for Computing 3-D Honeycomb Labyrinth Leakage*, ASME Paper GT2003-38238

Chougule H. H., Ramerth D., Ramachandran D., (2008): *Low Leakage Designs for Rotor Teeth and Honeycomb Lands in Labyrinth Seals*, ASME Paper GT2008-51024

Kang Y., Kim T. S., Kang S. Y., Moon H. K., (2010): *Aerodynamic Performance of Stepped Labyrinth Seals For Gas Turbine Applications*, ASME Paper GT2010-23256

Rosic B., Denton J. D., Curtis E. M., Peterson A. T., (2007): *The Influence of Shroud and Cavity Geometry on Turbine Performance – an Experimental and Computational Study, Part 2: Exit Cavity Geometry*, ASME Paper GT2007-27770

Rosic B., Denton J. D., (2006): *The Control of Shroud Leakage Loss by Reducing Circumferential Mixing*, ASME Paper GT2006-90946

Rudolph R., Sunshine R., Woodhall M., Haendler M., (2009): *Innovative Design Features of the SGT5-8000h Turbine And Secondary Air System*, ASME Paper GT2009-60137

Soemarwoto B. I., Kok J. C., de Cock K. M. J., Kloosterman A.B., Kool G.A., (2007): *Performance Evaluation of Gas Turbine Labyrinth Seals Using Computational Fluid Dynamics*, ASME Paper GT2007-27905

Vakili A. D., Meganathan A. J., Michaud M., Radhakrishnan S., (2005): *An Experimental and Numerical Study of Labyrinth Seal Flow*, ASME Paper GT2005-68224

Wróblewski W., Dykas S., Bochon K., Rulik S., (2010): *Optimization of Tip Seal With Honeycomb Land in LP Counter Rotating Gas Turbine Engine*, TASK Quarterly, Vol. 14/3, 189–207